Investigation of the Gas-Phase Kinetics of the Reaction K + SO_2 + Ar

A. Goumri, Dianna Laakso, John-David R. Rocha, Elizabeth Francis, and Paul Marshall*

Department of Chemistry, University of North Texas, P.O. Box 5068, Denton, Texas 76203-5068

Received: November 16, 1992; In Final Form: February 8, 1993

The recombination of atomic potassium, K(4^2S), with SO_2 has been investigated at about 863 K, in a bath of Ar at pressures from 20 to 690 mbar. K was generated by flash photolysis of KI vapor and monitored by time-resolved resonance absorption of a D-line at 766 nm under pseudo-first-order conditions. The measured pseudo-second-order rate constants lie in the low-pressure and falloff regions and were fitted with an empirical RRKM expression to yield $k_0 = 5.9 \times 10^{-29}$ cm^6 s^{-1} and $k_\infty = 6.2 \times 10^{-10}$ cm^3 s^{-1}. Error limits are discussed in the text. The KSO_2 adduct was characterized by *ab initio* methods. An RRKM analysis of k_0, together with a lower limit to the equilibrium constant, yielded a K–SO_2 bond strength of 190 ± 10 kJ mol^{-1}. k_∞ was shown to be consistent with a simple harpoon model for electron transfer.

1. Introduction

Molecular beam experiments by Ham and Kinsey showed that the interaction of atomic potassium, K(4^2S), with sulfur dioxide proceeds via formation of a long-lived complex.[1] The present study describes the first rate constant measurements of the recombination reaction

$$K + SO_2 (+ Ar) \rightarrow KSO_2 (+ Ar) \qquad (1)$$

carried out in the low-pressure and falloff regimes to obtain several kinds of information. The low-pressure limiting rate constant k_0 is employed with an RRKM analysis to estimate the K–SO_2 bond strength E_0, while an RRKM extrapolation to the high-pressure limit yields k_∞, which reflects the influence of long-range interactions between K and SO_2. These values are compared with those obtained in our earlier investigation[2] of

$$Na + SO_2 (+ Ar) \rightarrow NaSO_2 (+ Ar) \qquad (2)$$

These two reactions are examples of a general class in which metals form ionic adducts;[3-8] similar processes are important in combustion and atmospheric chemistry.[9-11] k_∞ for reaction 1 also provides a test of methods to predict k_∞ for other recombination reactions.

2. Experimental Technique

The concentration of atomic potassium was monitored by time-resolved atomic resonance absorption spectroscopy following its generation by pulsed UV photolysis of potassium iodide vapor in the presence of an excess of SO_2. Details of the methodology have been provided earlier,[2] so a brief summary is given here.

Mixtures of SO_2 diluted in a large excess of Ar bath gas were passed over a combustion boat containing KI, inside the stainless steel reactor which was heated to about 850 K. KI vapor was swept through the reaction zone, defined by the intersection region of the six arms of the reactor. The temperature inside the reaction zone was measured before and after each experiment with a moveable thermocouple, to an estimated accuracy of $\sigma_T/T \approx 2\%$. The bath gas served to maintain thermal equilibrium of the reactants and products, and slowed diffusion of K to the walls of the reactor. Previously we employed an excimer laser as the source of actinic radiation, but here atomic K was generated by flash-lamp photolysis through Suprasil optics. [K] was measured by the absorption of resonance radiation from a hollow-cathode lamp at a wavelength of 766 nm (K(4^2S) → K($4^2P_{3/2}$)) isolated with a monochromator. The transmitted light intensity, I, and the background value when [K] = 0, I_0, were measured with a red-sensitive Hamamatsu R-1477 photomultiplier tube: signals following up to 128 photolysis pulses were digitized and averaged before analysis. Fresh gas mixtures flowed through the reactor to replace the reagents and remove products between photolysis pulses (≈1-Hz repetition rate), with an average gas residence time of τ_{res} before the next photolysis pulse.

The absorption coefficient ϵ for atomic potassium and adherence to the Beer–Lambert law were examined in a separate apparatus. This consisted of a heated Pyrex tube with evacuated end windows (optical path length ≈ 11 cm) that contained potassium metal. The temperature was varied to change the vapor pressure of K and thus the transmittance of hollow-cathode radiation. We estimate $\epsilon \approx 2.6 \times 10^{-12}$ cm^2 atom^{-1}, which is similar to the value for Na,[4] as would be expected from the similar oscillator strengths.[12] The Beer–Lambert law was confirmed for transmittance down to 15%.[13]

Under the pseudo-first-order conditions employed we expect[2]

$$I = I_0 \exp[-\epsilon l [K]_0 \exp(-k_{ps1} t)] \qquad (3)$$

where t is time, l is the absorption path length, and k_{ps1} is the pseudo-first-order rate constant for loss of K:

$$-d[K]/dt = k_{ps2}[K][SO_2] + k_{diff}[K] = k_{ps1}[K] \qquad (4)$$

k_{ps2} is the pseudo-second-order rate constant for reaction 1, and k_{diff} accounts for the loss of K by processes other than reaction 1, primarily diffusion out of the reaction zone. k_{ps1} and the initial absorbance $\epsilon l[K]_0$ were obtained from about 2000 $I(t)$ points by nonlinear least-squares fitting,[5,14] typically at 5–12 values of [SO_2] from 0 to $[SO_2]_{max}$. k_{ps2} values, together with their precision σ_{kps2}, were derived from the slope of weighted linear plots of k_{ps1} vs [SO_2],[15] as shown in Figure 1.

3. Results

Twenty-three measurements of k_{ps2} are summarized in Table I. They were carried out at temperatures between 854 and 875 K, with a mean of 863 K and a standard deviation of 7 K. The total pressure was varied from nearly 20 to 700 mbar, corresponding to a variation of the total density [M] (effectively [Ar]) by a factor of 36. $[K]_0$ was varied from 0.5×10^{11} to 5.5×10^{11} cm^{-3} and τ_{res} from 0.2 to 5 s. There were no consistent variation of k_{ps2} with $[K]_0$ or τ_{res}, which indicates the absence of thermal decomposition of the SO_2 and that reaction 1 was successfully isolated from secondary processes.

Figure 2 shows k_{ps2} as a function of [M]. At [M] < 10^{18} cm^{-3} third-order behavior is observed, where $k_{ps2} \propto [M] = k_0[M]$, while at higher densities k_{ps2} lies in the falloff region. As discussed earlier in the case of reaction 2,[2] these observations can be interpreted in terms of a Lindemann mechanism where an initially

0022-3654/93/2097-5295$04.00/0

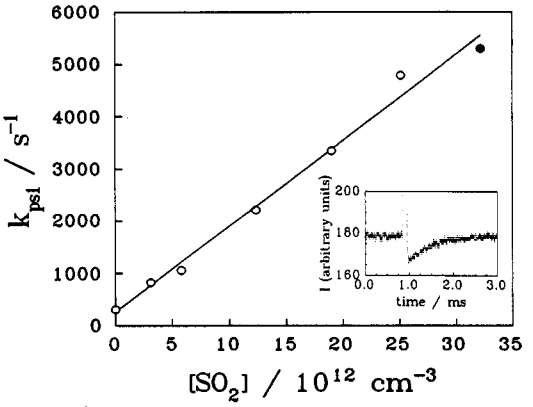

Figure 1. Plot of k_{ps1} for loss of K vs [SO_2] at P = 588 mbar. Inset shows a plot of the time-resolved transmitted light intensity, following flash photolysis at $t \approx 0.9$ ms, with [SO_2] = 3.2×10^{13} cm^{-3} (filled point).

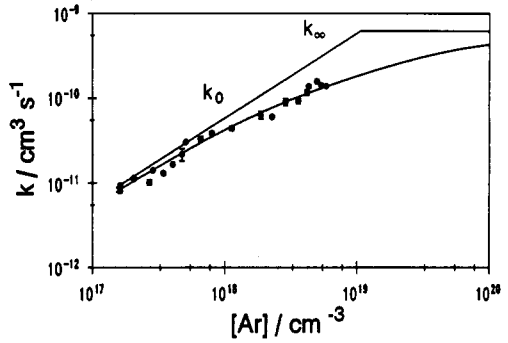

Figure 2. Plot of k_{ps2} for K + SO_2 vs [Ar] at 863 K, showing RRKM fit and limiting behavior at low (k_0) and high (k_∞) pressures.

TABLE I: Summary of Rate Constant Measurements for K + SO_2 + Ar at $T \approx 863$ K

P, mbar	[M] ≈ [Ar], 10^{17} cm^{-3}	τ_{res}, s	$[K]_0$, 10^{11} cm^{-3}	$[SO_2]_{max}$, 10^{13} cm^{-3}	$k_{ps2} \pm \sigma_{kps2}$, 10^{-11} cm^3 s^{-1}
19.5	1.62	0.3	1.3	2.8	0.933 ± 0.026
19.5	1.62	0.3	2.8	2.8	0.885 ± 0.036
19.5	1.62	0.3	5.5	2.8	0.803 ± 0.042
24.3	2.06	0.4	1.3	4.4	1.11 ± 0.03
24.3	2.06	0.4	2.8	4.4	1.14 ± 0.03
31.9	2.70	0.2	1.3	2.5	1.01 ± 0.07
33.9	2.87	0.5	1.9	3.5	1.40 ± 0.03
41.3	3.45	0.3	1.2	3.1	1.30 ± 0.06
47.9	4.06	0.7	0.7	5.3	1.65 ± 0.08
57.2	4.76	0.3	1.1	1.1	2.17 ± 0.36
61.1	5.09	0.3	1.0	2.7	3.03 ± 0.10
79.2	6.60	0.6	0.8	6.2	3.28 ± 0.25
96.3	8.02	0.4	0.7	3.8	3.84 ± 0.18
135	11.3	0.6	0.6	2.6	4.39 ± 0.24
224	18.7	1.7	1.0	3.5	6.32 ± 0.62
274	22.7	1.2	0.7	2.4	6.03 ± 0.22
339	28.7	1.5	1.0	3.3	9.06 ± 0.81
425	35.9	1.9	0.7	2.3	9.33 ± 0.66
495	41.9	3.7	1.1	2.6	11.7 ± 0.8
514	43.2	1.9	0.9	6.6	13.8 ± 0.6
588	49.8	2.7	0.5	3.2	15.8 ± 0.7
639	53.7	2.4	0.7	4.3	14.2 ± 0.6
692	58.6	5.2	2.7	5.6	13.9 ± 0.4

excited adduct is formed, which can either decompose back to reactants or be stabilized by collisions with the bath gas. Here we fit the empirical RRKM expression employed in the NASA rate constant compilation[16] to the data:

$$k_{ps2}(\text{NASA}) = \frac{k_0[\text{M}]}{1 + \frac{k_0[\text{M}]}{k_\infty}} 0.6^{[1 + (\log k_0[\text{M}]/k_\infty)^2]^{-1}} \quad (5)$$

We prefer eq 5 to the simpler Lindemann expression because that gives an unrealistically steep falloff of k_{ps2} with [M].[17] A nonlinear least-squares fit to the form of eq 5 yields the low- and high-pressure limiting rate constants, $k_0 = (5.9 \pm 0.3) \times 10^{-29}$ cm^6 s^{-1} and $k_\infty = (6.2 \pm 1.0) \times 10^{-10}$ cm^3 s^{-1}, respectively, where the uncertainties represent 1σ precision. This fit is shown in Figure 2, where it is extrapolated to high [M]. The root-mean-square deviation from the experimental data is 15%. Allowing for potential systematic errors, we estimate accuracy limits of ±20% for the fit.

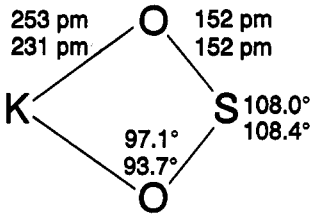

Figure 3. C_{2v} geometry for the KSO_2 adduct obtained with HF/3-21G* (upper) and HF/STO-3G* (lower) theory.

4. Discussion

***Ab Initio* Results.** The structure and vibrational frequencies of the KSO_2 adduct have been calculated by means of standard *ab initio* methods described by Hehre *et al.*[18] and implemented with the GAUSSIAN90[19] and GAMESS[20] programs. The geometries obtained at the Hartree–Fock level of theory with the STO-3G* and larger 3-21G* atomic basis sets are summarized in Figure 3, and the derived frequencies after scaling by a factor of 0.893 are 157, 335, 358, 585, 1124, and 1194 cm^{-1} (STO-3G*) and 152, 189, 234, 506, 971, and 1027 cm^{-1} (3-21G*). Results obtained with the larger basis set are expected to be more accurate and have been shown to give good accord with experiment for SO_2^-.[21] The geometry of the SO_2 fragment is similar to that of SO_2^- and in $NaSO_2$, which is established to be an ion-pair species.[3,21]

Low-Pressure Limit and K–SO_2 Bond Energy. There are two ways to derive the K–SO_2 bond dissociation enthalpy at 0 K, E_0. The first, kinetic method is based on the elementary processes:

$$\text{K} + \text{SO}_2 \rightleftarrows \text{KSO}_2^* \quad (6)$$

$$\text{KSO}_2^* + \text{M} \rightarrow \text{KSO}_2 + \text{M} \quad (7)$$

In the low-pressure limit $k_{-6} \gg k_7$, and the magnitude of the overall third-order rate constant for consumption of K, k_0, is determined by the ratio k_7/k_{-6}. k_7 can be estimated reasonably and thus E_0 is obtainable, since as E_0 increases k_{-6} becomes larger, because of the greater density states in the adduct. This analysis is independent of the subsequent fate of the KSO_2 formed in the stabilization step 7. Collisional quenching by Ar makes the lifetime of KSO_2* so short, on the order of 10^{-8} s, that [KSO_2*] is unaffected by any secondary chemistry.

We showed earlier that, on the basis of the RRKM formalism of Troe,[22,23] k_0 can be expressed in terms of fundamental properties of K, SO_2, and KSO_2

$$k_0 = \beta_c Z_{LJ} \frac{\rho(E_0)RT}{Q_{vib}(\text{KSO}_2)} F_E F_{anh} F_{rot} \frac{Q(\text{KSO}_2)}{Q(\text{K})Q(\text{SO}_2)} \quad (8)$$

where $\beta_c Z_{LJ}$ is the weak-collision stabilization rate constant, assumed to be 2×10^{-10} cm^3 s^{-1}, $\rho(E_0)$ is the vibrational density of states of KSO_2 at the threshold energy E_0 for dissociation, the Qs are the partition functions, and F_E, F_{anh}, and F_{rot} are factors to account for the energy dependence of $\rho(E_0)$, for the effects of vibrational anharmonicity, and for centrifugal barriers and are estimated to be 1.21, 1.37, and 6.9, respectively. Q values for SO_2 and KSO_2 are derived from theoretical HF/3-21G* data, with the assumption that the electronic partition function for the $^2A''$ adduct is 2. $\rho(E_0)$ and to a minor degree F_E and F_{rot} are functions of E_0, which was varied until agreement with the measured k_0 was obtained for E_0 = 176 kJ mol^{-1}. We allow for

a factor of 2 uncertainty in eq 8, which leads to an uncertainty of ±25 kJ mol^{-1} in E_0.

An alternative thermodynamic assessment of E_0 is based on the observation that even at the smallest [SO_2] employed all of the K appeared to be consumed rapidly, i.e., the equilibrium constant K_{eq} for reaction 1 is large. On the conservative assumption that for [SO_2] = 5×10^{12} cm^{-3} at least half the K is removed by reaction 1 rather than diffusion, a lower limit to K_{eq} is 2×10^{-13} cm^3. Using the statistical mechanical result[24]

$$K_{eq} = \frac{Q(KSO_2)}{Q(K)Q(SO_2)} \exp\left(\frac{E_0}{RT}\right) \quad (9)$$

this implies $E_0 > 180$ kJ mol^{-1}, which is consistent with the E_0 derived from the RRKM analysis above. The apparent value of K_{eq} is vulnerable to any subsequent removal of KSO_2 by other chemistry which might prevent accumulation of KSO_2 and attainment of equilibrium, e.g., reaction of KSO_2 with atomic iodine. While the amount of I generated photolytically is insufficient to affect [KSO_2] significantly, it is possible that heterogeneous reactions between KI and SO_2 liberate I in greater concentrations, although no evidence for this was seen. Thus, the thermodynamic limiting value is itself an upper limit.

Combination of the kinetic and thermodynamic estimates of E_0 leads to $E_0 \approx 190 \pm 11$ kJ mol^{-1}. This the same as our earlier estimate of the Na–SO_2 bond strength as 190 ± 15 kJ mol^{-1} by means of similar arguments,[2] which is in excellent accord with flame modeling which yielded 197 ± 20 or 210 ± 20 kJ mol^{-1}.[9,25] k_0 is greater for K + SO_2 than for Na + SO_2 because the alkali metal–oxygen stretching frequencies are lower in the adduct formed from the heavier metal, and so the density of states is higher in reaction 1 than in reaction 2. The E_0 values for Na–SO_2 and K–SO_2 lie within the range of Na–O_2 and K–O_2 bond strengths proposed from a variety of experimental and theoretical work on alkali metal superoxides, 150–250 kJ mol^{-1}, where several usually reliable methods show as yet unresolved disagreements.[26]

High-Pressure Limit. At the high-pressure limit $k_7 \gg k_{-6}$, and the overall second-order rate constant for removal of K, k_∞, is equal to k_6. k_∞ can be predicted on the assumption that the rate of association of K with SO_2 is controlled by passage over the centrifugal barrier in an attractive potential of the form $V(r) = -C_6/r^6$.[27] C_6 is estimated to be 6.54×10^{-77} J m^6 from polarizability data for K and SO_2,[28] which leads to a reaction cross-section of 0.91 nm^2. Multiplication by the average relative velocity of K and SO_2 at 863 K, 869 m s^{-1}, yields $k_\infty = 8.0 \times 10^{-10}$ cm^3 s^{-1}. For comparison, a similar analysis for reaction 2 led to a slightly larger k_∞ of 8.5×10^{-10} cm^{-3} s^{-1} at 787 K.[2]

An alternative calculation is based on the simple harpoon model[29] for electron transfer from K to SO_2, with an ionization potential for K of 419 kJ mol^{-1} and an electron affinity for SO_2 of 107 kJ mol^{-1}.[30,31] This model indicates that the K^+–SO_2^- configuration is favored for separations of up to 0.45 nm, which corresponds to a cross-section of 0.62 nm^2 and $k_\infty = 5.4 \times 10^{-10}$ cm^3 s^{-1}. For Na + SO_2 the harpoon model yielded $k_\infty = 4.0 \times 10^{-10}$ cm^3 s^{-1},[2] which is smaller because of the higher ionization potential of Na relative to K.

Both estimates of k_∞ for reaction 1 are close to the experimental value of about 6×10^{-10} cm^3 s^{-1}, but only the harpoon model correctly predicts a reduction in k_∞ for reaction 2, for which we earlier estimated $k_\infty \approx 3 \times 10^{-10}$ cm^3 s^{-1}.[2] Thus, long-range electron transfer appears to be the dominant factor that determines the high-pressure limit in these addition reactions.

5. Conclusions

Rate constants for the addition of K to SO_2 have been measured in the low-pressure and falloff regimes and can be fitted with an empirical RRKM expression. The low-pressure limiting rate constant, combined with *ab initio* information for the adduct, yields the K–SO_2 bond strength. The high-pressure limit is consistent with the idea that long-range electron transfer is the rate-limiting process for initial adduct formation.

Acknowledgment. We thank R. Ramirez and J. A. White for technical assistance. This work was supported by the Robert A. Welch Foundation (Grant B-1174), the U.N.T. Organized Research Fund, and the Texas Academy of Mathematics and Science. Some of the computer time was provided by the NSF Pittsburgh Supercomputing Center (Grant CHE900059P).

References and Notes

(1) Ham, D. O.; Kinsey, J. L. *J. Chem. Phys.* **1968**, *48*, 939.
(2) Shi, Y.; Marshall, P. *J. Phys. Chem.* **1991**, *95*, 1654.
(3) Milligan, D. E.; Jacox, M. E. *J. Chem. Phys.* **1971**, *55*, 1003.
(4) Marshall, P.; Narayan, A. S.; Fontijn, A. *J. Phys. Chem.* **1990**, *94*, 2998.
(5) Husain, D.; Marshall, P.; Plane, J. M. C. *J. Chem. Soc., Faraday Trans. 2* **1985**, *81*, 301.
(6) Silver, J. A.; Zahniser, M. S.; Stanton, A. C.; Kolb, C. E. *20th Symposium (International) on Combustion*; The Combustion Institute: Pittsburgh, PA, 1984; p 605.
(7) Plane, J. M. C.; Rajasekhar, B. *J. Phys. Chem.* **1989**, *93*, 3135.
(8) Husain, D.; Plane, J. M. C.; Xiang, C. C. *J. Chem. Soc., Faraday Trans. 2* **1984**, *80*, 1619.
(9) Steinberg, M.; Schofield, K. *Prog. Energy Combust. Sci.* **1990**, *16*, 311.
(10) Fontijn, A. *Combust. Sci. Technol.* **1986**, *50*, 151.
(11) Plane, J. M. C. *Int. Rev. Phys. Chem.* **1991**, *10*, 55.
(12) Wiese, W. L.; Smith, M. W.; Miles, B. M. *Atomic Transition Probabilities*; National Bureau of Standards NSRDS-NBS 22: Washington, DC, 1969; Vol. 2.
(13) Because the absolute [K] in the calibration cell is sensitive to the precise temperature, our ϵ is uncertain perhaps by a factor of 2. However, knowledge of the absolute [K] is not required for the kinetic analysis. Our results are apparently at odds with a similar calibration for unresolved D-lines reported by Husain and Plane (*J. Chem. Soc., Faraday Trans. 2* **1981**, *78*, 1175), who employed an AC potassium spectral lamp and noted non-Beer–Lambert behavior with an implied ϵ of the order of 3×10^{-15} cm^2 $atom^{-1}$. Consistent with this, a comparison of the absorbance by K in our kinetic reactor of resonance radiation from both hollow-cathode and AC lamps showed that the effective ϵ for the AC lamp was much smaller than that for the hollow-cathode lamp. Line reversal in the AC lamp might account for the different behavior.
(14) Marshall, P. Ph.D. Thesis, University of Cambridge, 1985.
(15) Irvin, J. A.; Quickenden, T. I. *J. Chem. Educ.* **1983**, *60*, 711.
(16) DeMore, W. B.; Molina, M. J.; Sander, S. P.; Golden, D. M.; Hampson, R. F.; Kurylo, M. J.; Howard, C. J.; Ravishankara, A. R. *Chemical Kinetics and Photochemical Data for Use in Stratospheric Modeling. Evaluation Number 8*; JPL Publication of 87-41; Jet Propulsion Laboratory: Pasadena, CA, 1987.
(17) Robinson, P. J.; Holbrook, K. A. *Unimolecular Reactions*; Wiley-Interscience: London, 1972; Chapter 1.
(18) Hehre, W. J.; Radom, L.; Schleyer, P. v. R.; Pople, J. A. *Ab Initio Molecular Orbital Theory*; Wiley: New York, 1986.
(19) Frisch, M. J.; Head-Gordon, M.; Trucks, G. W.; Foresman, J. B.; Schlegel, H. B.; Raghavachari, K.; Robb, M. A.; Binkley, J. S.; Gonzalez, C.; Defrees, D. J.; Fox, D. J.; Whiteside, R. A.; Seeger, R.; Melius, C. F.; Baker, J.; Martin, R. L.; Kahn, L. R.; Stewart, J. J. P.; Topiol, S.; Pople, J. A. *Gaussian 90*; Gaussian: Pittsburgh, PA, 1990.
(20) Schmidt, M. W.; Baldridge, K. K.; Boatz, J. A.; Jensen, J. H.; Koseki, S.; Gordon, M. S.; Nguyen, K. A.; Windus, T. L.; Elbert, S. T. *QCPE Bull.* **1990**, *10*, 52.
(21) Ramondo, F.; Bencivenni, L. *Mol. Phys.* **1989**, *67*, 707.
(22) Troe, J. *J. Phys. Chem.* **1979**, *83*, 114.
(23) Troe, J. *J. Chem. Phys.* **1981**, *75*, 226.
(24) Pitzer, K. S.; Brewer, L. *Thermodynamics*, 2nd ed.; McGraw-Hill: New York, 1961; Chapter 27.
(25) Schofield, K.; Steinberg, M. *J. Phys. Chem.* **1992**, *96*, 715.
(26) Schofield, K. In *Gas-Phase Metal Reactions*; Fontijn, A., Ed.; North-Holland: Amsterdam, 1992; Chapter 23.
(27) Rogowski, D. F.; Marshall, P.; Fontijn, A. *J. Phys. Chem.* **1989**, *93*, 1118.
(28) Lide, D. R. *CRC Handbook of Chemistry and Physics*, 71st ed.; CRC Press: Boca Raton, FL, 1990.
(29) Magee, J. L. *J. Chem. Phys.* **1940**, *8*, 687.
(30) Chase, M. W., Jr.; Davies, C. A.; Downey, J. R., Jr.; Frurip, D. J.; McDonald, R. A.; Syverud, A. N. JANAF Thermochemical Tables, 3rd ed. *J. Phys. Chem. Ref. Data* **1985**, *14*, Suppl. 1.
(31) Nimlos, M. R.; Ellison, G. B. *J. Phys. Chem.* **1986**, *90*, 2574.